Hybridization of GNSS Receivers with INS Systems for Terrestrial Applications in Airport Environment

Guglielmo Casale*, Patrizio De Marco*, Romano Fantacci**, Simone Menci**

* Selex - Sistemi Integrati - ATM & Airport Systems Division
Via Tiburtina Km 12.4 Rome - 00131 Italy
Phone: +39-06-4150.3976, Fax: +39-06-4150.3728
e-mail: gcasale@selex-si.com, pdemarco@selex-si.com
** University of Florence – Department of Electronics and Telecommunications
Via di S. Marta 3 Florence – 50139 Italy
Phone: +39-0554796467, Fax: +39-0554796485
e-mail: fantacci@lart.det.unifi.it, menci@lart.det.unifi.it

Abstract. This paper deals with the study of low-cost efficient techniques of GNSS-INS integration for the realization of a surveillance system for the terrestrial vehicular traffic in an airport. This system will have to enable accurate, continuous and reliable tracking of each ground vehicle operating in airport area in support of maintenance and management of aircrafts. High accuracies are required to give the ground control a precise and dynamic view of the airport situation, in order to optimize the ATM (Air Traffic Management) activity; this is particularly important in large hubs. In order to integrate satellites and sensors measurements we relied on Kalman filtering, a powerful signal processing tool for optimal blending of heterogeneous data sources. Specifically, we used an integration architecture named tightly coupled, where only one Kalman filter is used to integrate pseudorange, Doppler and sensor measurements. We will show that our hybrid receiver is a rather simple but extremely efficient solution to this problem.

1 Introduction

One of the main drawbacks of using GNSS (*Global Navigation Satellite Systems*) systems like GPS, GLONASS or Galileo for land surveying, navigation (mainly terrestrial) and in general route tracking, is the temporary loss of service we get when the receiver is moving under bridges or other types of obstacles. For example, a terrestrial vehicle equipped with a GPS receiver would experiment a loss of positioning when passing under trees surrounding the street; in the same way an aircraft flying at low altitude above that vehicle or standing still in its proximity, not so rare events in an airport environment, could produce the same effect. In these cases the obstacles are responsible of partial or total obstruction of the satellites navigation signals, and, during these service outages, navigation performance degrades rapidly. So one of the main problems of stand-alone satellite navigation is the service continuity, which is not guaranteed in all application scenarios. Various techniques may be used to compensate this drawback: one of the most important classes goes under name

of *data fusion* (or data integration), that is the combination of the information coming from GNSS measurements with that coming from other sensors (vehicular or not) which are not affected by the above mentioned vulnerabilities.

A simple system of this type consists of using the technique, well known to navigators, named *"dead reckoning"* which, in its most simple realization, takes advantage of an odometer and a magnetic compass (or a system of gyroscopes for a three-dimensional system) which measurements are integrated with GNSS measurements in order to assist the receiver in the interpolation of vehicle position during the loss of tracking of satellites. But, in a more general view, the information may also come from accelerometers, tachometers, altimeters, and from any other instrument suited to the application and mounted on the vehicle considered. The most sophisticated approaches involve combining GNSS with INS (*Inertial Navigation Systems*): these systems are usually made of gyroscopes for the determination of the angular motion of vehicle axes with respect to a local reference system and of accelerometers oriented along these axes to measure the accelerations. Starting from a known position and twice integrating in time the accelerations we obtain differences of position that determine the vehicle trajectory, along with its velocity, acceleration and attitude. The simple sensor group that realizes dead reckoning for a terrestrial vehicle can be viewed like a simplified form of INS platform [1].

Inertial systems have some advantages with respect to GNSS: they are autonomous and independent from external sources, they have not visibility problems, and often provide accuracies similar to GNSS when used in short time intervals. *Hence, INS can be used as an interpolator for gaps of service in GNSS*. As a drawback, the estimation error tends to grow with a quadratic trend in time because of sensor errors, hence periodic resets with known and accurate positions are required in order to prevent excessive degradations of the position estimate. Indeed sensors are not ideal, they are affected by noise and distortions, so inertial navigation performance depends strongly from their quality (and hence their cost) [2].

So, GNSS and INS systems have complementary characteristics that render them ideal candidates for the integration. In fact GNSS periodically reinitializes INS, and this last one integrates GNSS during outage periods and assists it in satellites tracking.

This paper deals with the study of low-cost efficient techniques of GNSS-INS integration for the realization of a surveillance system for the terrestrial vehicular traffic in an airport. This system will have to enable accurate, continuous and reliable tracking of each ground vehicle operating in airport area in support of maintenance and management of aircrafts (refuelling, maintenance, baggage transport, safety, etc.). Each vehicle equipped with hybrid receiver will then transmit its position to the airport control room, where the operator will be able to monitor the overall situation and dispatch orders. For these transmissions we don't assume any particular technology; good candidates are the Extended Squitter channel on 1090 MHz frequency or a wireless link realized with Wi-Fi or WiMAX technologies.

High accuracies are required to give the ground control a precise and dynamic view of the airport situation, in order to optimize the ATM (*Air Traffic Management*) activity; this is particularly important in large hubs. It's clear that this objective can be reached only through full continuity of positioning service.

In the continuation of this paper, we will assume a GPS / EGNOS receiver for reasons of rapid implementation, but it's important to point out that these results may be easily extended in a straightforward way to future multisystem GNSS receivers.

2 System Architecture

We can count at least three different architectures for GPS / INS integration [1,2]: they are depicted in Fig. 1. Modes a) (*uncoupled mode*) and b) (*loosely coupled*) initially consider GPS receiver and INS like separate systems and then integrate "optimally" the measures of position, velocity and attitude keeping count of the respective estimation error variances. Mode c) (*tightly coupled*) instead considers GPS and INS like "virtual sensors", that is systems which outputs measurements of pseudorange, pseudorange rate (or, equivalently, Doppler shifts) and variations of velocity and heading. In this case there is only one navigation processor responsible of fusion of all data, obviously more complex than the other cases. The tightly coupled approach is the one we chose, because while it's the more complex to study and implement, it's also potentially the more performance effective.

In order to integrate satellite and sensors measurements we relied on *Extended Kalman Filter (EKF)* [2,3], a powerful signal processing tool for optimal blending of heterogeneous data sources. With tightly coupled architecture only one EKF is used to integrate pseudorange and Doppler satellite and sensor measurements. In general, Kalman filtering allows to optimally estimate the state x_k of a dynamic system based on measurements z_k (at discrete-time step t_k) and on uncertain system dynamic model:

$$x_{k+1} = \Phi_k x_k + G_k u_k + \Gamma v_k$$
$$z_k = H_k x_k + w_k$$

The first equation is the *dynamic equation*, while the second is the *measurement equation*. v_k is the *process noise*, here an acceleration noise, which models uncertainty on

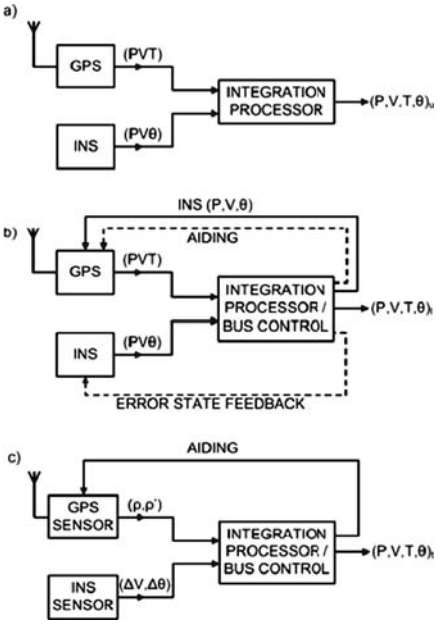

Fig. 1. Generic architecture GPS/INS: a) uncoupled mode; b) loosely coupled mode; c) tightly coupled mode.

Table 1. Essential equations of extended kalman filter.

Predictor (time updates)
Predicted State Vector
$\hat{x}_k^- = \Phi_k \hat{x}_{k-1}^+$
Predicted Covariance Matrix
$P_k^- = \Phi_k P_{k-1}^- \Phi_k^T + Q_{k-1}$
Corrector (measurements updates)
Kalman Gain
$\bar{K}_k = P_k^- H_k^T (H_k P_k^- H_k^T + R_k)^{-1}$
Corrected State Estimation
$\hat{x}_k^+ = \hat{x}_k^- + \bar{K}_K (z_k - H_k \hat{x}_k^-)$
Corrected Covariance Matrix
$P_k^+ = P_k^- - \bar{K}_K H_k P_k^-$

dynamic system model, w_k is the *measurement noise*, which models pseudorange and Doppler measurement errors and sensors errors. Γ is a *noise distribution matrix*, which keeps count of impact of acceleration noise on all state variables. In our system we have no control input u_k, so we will neglect it. The equations that compose EKF are reported in Table 1 with following explanation of quantities and symbols.
where:

Φ_k is the *state transition matrix*.
H_k is the *measurement sensitivity matrix* or *observation matrix*.
$H_k \hat{x}_k^-$ is the *predicted measurement*.
$z_k - H_k \hat{x}_k^-$, the difference between the measurement vector and the predicted measurement, is the *innovations vector*.
$\bar{K}_K$ is the *Kalman gain*.
P_k^- is the *predicted* value or *a priori* of estimation covariance.
P_k^+ is the *corrected* value or *a posteriori* of estimation covariance.
Q_k is the covariance of dynamic disturbance noise.
R_k is the covariance of *sensor noise* or *measurement uncertainty*.
$\hat{x}_k^-$ is the *predicted* or *a priori* value of the estimated state vector.
$\hat{x}_k^+$ is the *corrected* or *a posteriori* value of the estimated state vector.
z_k is the *measurement vector* or *observation vector*.

We chose the following state vector, taking into account two components (along East and North) of horizontal position, velocity and acceleration, and the errors typically associated with receiver clock, bias and drift.

$$x_k = \left[\Delta \mathrm{P}_E \; \Delta \mathrm{P}_N \; \Delta \mathrm{V}_E \; \Delta \mathrm{V}_N \; \Delta \mathrm{A}_E \; \Delta \mathrm{A}_N \; b \; d\right]^T$$

We assumed that in a airport environment (with terrain almost flat) a terrestrial vehicle has only two significant degree of freedom: longitudinal translation (about roll axis) and azimutal rotation (about yaw axis), that is, as a good approximation, we neglected other types of movements. So, we used only two sensors: an accelerometer and a gyroscope.

Table 2. GPS/EGNOS receiver, sensor models and indicative costs.

Reference GPS receiver	u-blox TIM-LR	Chipset 70–80 €
Accelerometer	Analog Devices ADXL 103	7–8 $
Gyroscope	Analog Devices ADXRS 150	30 $

The specific GPS receiver and sensors models assumed in this work are shown in Table 2 [4,5].

It's important to remark that all these components were chosen to have low costs in order to make feasible the implementation of the entire system even in a large airport with many vehicles. Moreover, the inertial sensors are realized with MEMS (*MicroElectroMechanical Systems*) technology, hence they have very interesting characteristics. Next, we summarize the main of them:

- Good performance
- Low cost
- Very low weight, dimensions, power consumption and dissipated heat, so they are well suited for installation on various types of mobile platforms.

The GPS receiver is conceived for integrated applications, because is predisposed to accept sensor inputs and is equipped with EKF software for dead reckoning applications; it supports fully automatic calibration of sensor inputs with temperature compensation and it has a 40 Hz dead reckoning calculation rate for high accuracy calculations (we will see later that this is a very important parameter). The position update rate is 1 Hz.

This receiver can also receive EGNOS signals for the application of differential corrections in order to have integrity and accuracy improvements [6]. We will exploit this capability in order to maximize performance.

After some filter tuning [3], we managed to find the optimal choice for the above mentioned vectors and matrices, here reported:

Initial state estimate and associated covariance matrix:

$$x_0 = \vec{0} \quad P_0^+ = diag\left(8.46^2, 8.46^2, 10^{-3}, 10^{-3}, 10^{-3}, 10^{-3}, 10^4, (c \cdot 10^{-6})^2\right)$$

(all lengths are expressed in km)

Matrices related to dynamic equation:

$$\Phi_k = \left[\begin{array}{cccccc|cc} 1 & 0 & T & 0 & T^2/2 & 0 & 0 & 0 \\ 0 & 1 & 0 & T & 0 & T^2/2 & 0 & 0 \\ 0 & 0 & 1 & 0 & T & 0 & 0 & 0 \\ 0 & 0 & 0 & 1 & 0 & T & 0 & 0 \\ 0 & 0 & 0 & 0 & 1 & 0 & 0 & 0 \\ 0 & 0 & 0 & 0 & 0 & 1 & 0 & 0 \\ \hline 0 & 0 & 0 & 0 & 0 & 0 & 1 & T \\ 0 & 0 & 0 & 0 & 0 & 0 & 0 & 1 \end{array}\right] \qquad \Gamma = \left[\begin{array}{c} T^2/2 \\ T \\ 1 \end{array}\right]$$

$$Q_{k-1} = \Gamma \sigma_\nu^2 \Gamma^T = \left[\begin{array}{cccccc|cc} T^4/4 & 0 & T^3/2 & 0 & T^2/2 & 0 & 0 & 0 \\ 0 & T^4/4 & 0 & T^3/2 & 0 & T^2/2 & 0 & 0 \\ T^3/2 & 0 & T^2 & 0 & T & 0 & 0 & 0 \\ 0 & T^3/2 & 0 & T^2 & 0 & T & 0 & 0 \\ T^2/2 & 0 & T & 0 & 1 & 0 & 0 & 0 \\ 0 & T^2/2 & 0 & T & 0 & 1 & 0 & 0 \\ \hline 0 & 0 & 0 & 0 & 0 & 0 & Q_b & Q_{bf} \\ 0 & 0 & 0 & 0 & 0 & 0 & Q_{bf} & Q_f \end{array}\right] \sigma_v^2$$

The process noise is a DWPA (Discrete-time Wiener Process Acceleration), hence with white noise acceleration increments (*jerk*).

Matrices related to measurement equation:

$$z_k = \begin{bmatrix} PR_{s1} \\ \vdots \\ PR_{sM} \\ \hline D_{s1} \\ \vdots \\ D_{sM} \\ \hline a_r \\ \phi_y \end{bmatrix} \quad H_k = \left[\begin{array}{cccccc|cc} -e_{E1} & -e_{N1} & 0 & 0 & 0 & 0 & 1 & T \\ \vdots & \vdots & \vdots & \vdots & \vdots & \vdots & \vdots & \vdots \\ -e_{EM} & -e_{NM} & 0 & 0 & 0 & 0 & 1 & T \\ \hline 0 & 0 & -e_{E1} & -e_{N1} & 0 & 0 & 0 & 1 \\ \vdots & \vdots & \vdots & \vdots & \vdots & \vdots & \vdots & \vdots \\ 0 & 0 & -e_{EM} & -e_{NM} & 0 & 0 & 0 & 1 \\ \hline 0 & 0 & 0 & 0 & a_{Er} & a_{Nr} & 0 & 0 \\ 0 & 0 & 0 & 0 & a_{Ey} & a_{Ny} & 0 & 0 \end{array}\right]$$

$$R_k = diag\left(\sigma_{PR1}^2, \cdots, \sigma_{PRM}^2, \sigma_{D1}^2, \cdots, \sigma_{DM}^2, \sigma_a^2, \sigma_\phi^2\right)$$

where e_{Ei} and e_{Ni} are the components along East and North axis (of local tangent plane (LTP)) of unit vectors pointing i-th satellite from receiver position; PR_{si} and D_{si} are respectively pseudorange and pseudorange rate (derived from Doppler) measurements, a_r and φ_y are the sensors measurements, respectively roll axis acceleration and yaw axis rotation.

In order to better understand how sensors sensibilities terms a_{Er}, a_{Nr}, a_{Ey} and a_{Ny} are calculated, we recall here the basis of dead reckoning navigation. In Fig. 2 the basic analytical formulation of dead reckoning navigation is depicted. We will initially refer to the classical formulation where vehicle is equipped with an odometer for measurement of distance travelled Δl_i and a magnetic compass / gyroscope for measurement of variation of heading θ_i in the i-th time interval ΔT (fixed or variable sampling time).

Coordinates X and Y define the horizontal plane where the vehicle moves in a trajectory from initial point (X_0, Y_0) to destination (X_n, Y_n) (X maybe East coordinate,

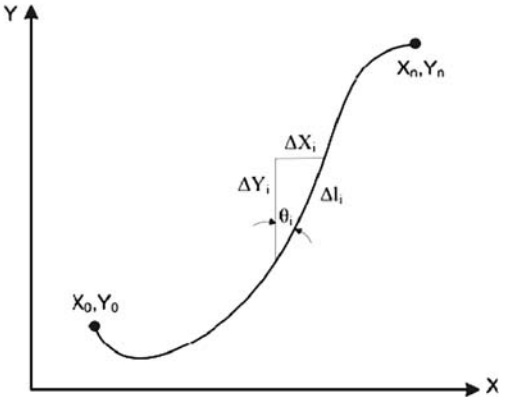

Fig. 2. Dead reckoning formulation.

Y maybe North). For each sampling interval, the vehicle's autonomous navigation unit updates its position with the following first-order approximation:

$$X_n = X_0 + \sum_1^n \Delta X_i = X_0 + \sum_1^n \Delta l_i \sin\theta_i$$

$$Y_n = Y_0 + \sum_1^n \Delta Y_i = Y_0 + \sum_1^n \Delta l_i \cos\theta_i$$

In this way, the reconstructed trajectory is a first-order approximation of the real trajectory, that is a piecewise linear curve. Clearly, the quality of position estimation depends from sampling time and sensors measurement errors, since position errors tend to grow in time because of sensor errors. Odometers are today present on vehicles equipped with ABS, while heading sensors may be implemented with a magnetic compass. The problem is that odometers and compasses yield measurements subjected to serious error effects, like noise, bias, drift and distortion.

We use this formulation for dead reckoning implementation, but in a slightly modified way in order to use more precise sensors like the accelerometers and gyroscopes we chose.

So, starting with geometric relations:

$$a_E = a_r \sin(\phi_y) \quad a_N = a_r \cos(\phi_y)$$

inverting these and taking partial derivatives w. r. t. a_E and a_N, we obtain:

$$a_{Er} = a_E / a_r \quad a_{Nr} = a_N / a_r$$
$$a_{Ey} = a_N / a_r^2 \quad a_{Ny} = -a_E / a_r^2$$

which must be calculated using the filter actual better state estimate.

Before Kalman integration we used a particular smoothing procedure of GPS measurements, the *Hatch filter*, which combines pseudorange and Doppler measurements to reduce the effect of multipath and receiver noise.

2.1 Pseudorange Smoothing Filter

In steady state, each L1 pseudorange measurement from GPS receiver is smoothed using the filter:

$$PR_s(k) = \left(\frac{1}{N}\right) PR_r(k) + \left(\frac{N-1}{N}\right)\left[PR_s(k-1) + \phi(k) - \phi(k-1)\right]$$
$$N = S/T$$

where

PR_r is the raw pseudorange,
PR_s is the smoothed pseudorange,
N is the number of samples,
S is the time filter constant, equal to 100 seconds,
T is the filter sample interval, nominally equal to 0.5 seconds and not to exceed 1 second,
ϕ is the accumulated phase measurement,
k is the current measurement, and
$k-1$ is the previous measurement.

In principle the more epochs of data are used in the smoothing process the more precise the smoothed pseudorange should become, and should approach the precision of the carrier range (mm-level). In practice there are facts which destroy this ideal situation:

- Since the ionosphere delays the pseudorange and advances the carrier range the change in pseudorange does not equal exactly the change in carrier range (this effect is called the ionospheric divergence).
- If the receiver channel looses lock on the SV momentarily, or if the range rate of change is too high, the carrier phase integration process is disrupted, resulting in a "cycle slip", and an incorrect change in carrier range.

To overcome the above drawbacks the number of observations used to smooth the pseudoranges is limited. At one observation per second a maximum of 100 is a good value. Moreover, large cycle slips can be detected: if the carrier rate of change is larger by a certain margin than the pseudorange rate of change, a cycle slip is declared and the smoothing algorithm is reset (n = 1). The margin depends very much on the noise and multipath figures of the receiver and the antenna location. For high quality receivers with optimally located antennas the margin could be as low as 1 m, a value of 15 m is more realistic, which implies that slips of more than 100 cycles (1 cycle is about 0.2 m) remain undetected. The limit value for N limits the error in the smoothed pseudorange, and lets it fade away after one to two minutes.

Code smoothing reduces multipath and receiver noise on the pseudoranges. Although theoretically a reduction of a factor 10 can be reached, we can count on a practical reduction of at least a factor 2, and up to 5. An example of benefit of using this filter is depicted in Fig. 5, where we can see that really the accuracy improvement we get is described by a factor from 2 to 5. We chose this particular smoothing filter in order to further improve estimation accuracy because of its simplicity and cheapness that makes it very attractive to implement.

3 Simulation Scenario

Our activity was carried out through computer simulations with a flexible satellite navigation software simulator.

The simulations involved a vehicle moving in the Roma-Fiumicino airport (Fig. 3); the service vehicle's route (Fig. 4) describes a movement from head of 16R runway to the terminal area. The trajectory is a piecewise linear curve with distributed accelerations and decelerations and changes of heading concentrated in specific waypoints. These particular trajectory, along with accelerations and speed values, is studied to be slighter "extreme" than a realistic case, in order to test satellite tracking and system performance in a sort of "worst case". This route has a length of 4.89 km and, with assumed speeds, the receiver moves from waypoint 1 to waypoint 15 in about 4 minutes; the first part (till waypoint 7) is fairly straight, while second part is much more articulated with more frequent changes of directions, accelerations and decelerations.

Monte Carlo simulations were performed in order to reduce the variability of stochastic factors on position and velocity estimates.

Simulations were made with 11 GPS satellites and the 3 EGNOS satellites all visible from the receiver, a fairly good condition for receiver performance.

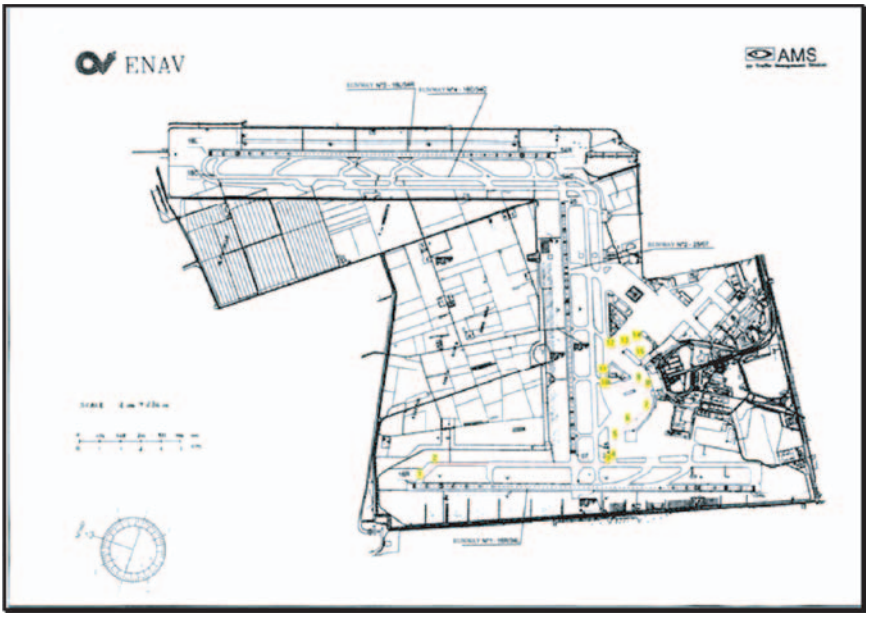

Fig. 3. Roma-fiumicino airport.

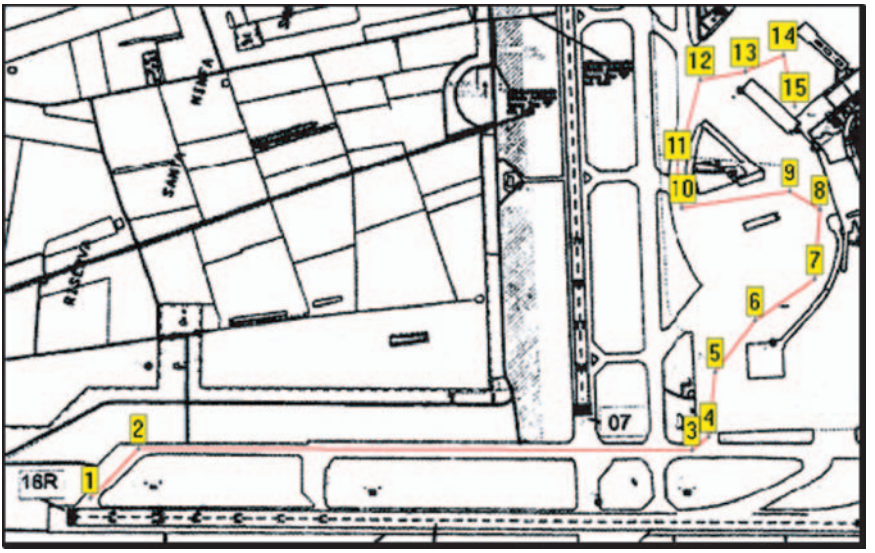

Fig. 4. Route chosen for simulation purposes.

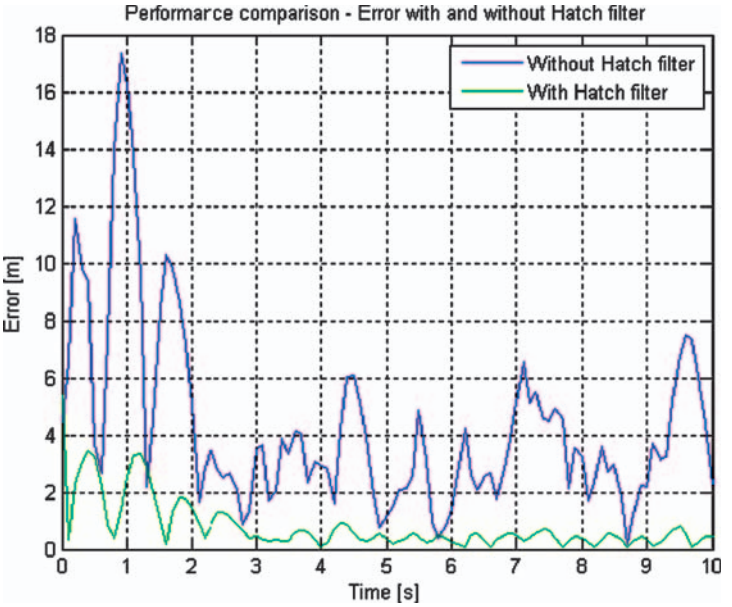

Fig. 5. Improving positioning error through use of Hatch filter.

4 Experimental Results

Next, we see some results obtained from simulations. We set, as the main performance parameter, a target HPL (*Horizontal Protection Level*) of 5 m; *the instantaneous horizontal position estimation error (and its RMS value) must be lower than this threshold in order to declare satisfying navigation performance*. Moreover, we evaluated the *service availability (SA)*, that is *the percentage of time that estimation error is in this acceptable error range*; this parameter must be ≥ 99.5% in order to be satisfying.

Figure 6 shows a plot of estimation error for vehicle movement along the entire chosen route: we can see that GPS stand-alone is not capable of guarantee the target performance in every time, even with many visible satellites and the presence of EGNOS: this is also due to the vehicle dynamic, in fact the error spikes correspond to the turns showed in Fig. 4, more frequent in the second half of route. Though the RMS error is only 2.751 m, the SA is only 81.2%, an unacceptable performance. Instead, hybrid receiver is always capable of maintaining error lower than 3 m, with an RMS error of 0.960 m and a 100% SA, even in cases of rapid unexpected turns, and this is the effect of the sensors presence and of the highest frequency of computing carried out on their measurements with respect to GPS observations.

Figure 7 depicts first 30 s of a situation in which we have a partial loss of tracking (only 6 satellites are visible, with a bad geometry) from 10 s to 20 s. This situation is related to the vehicle passing under an extended obstacle or near a building, and has

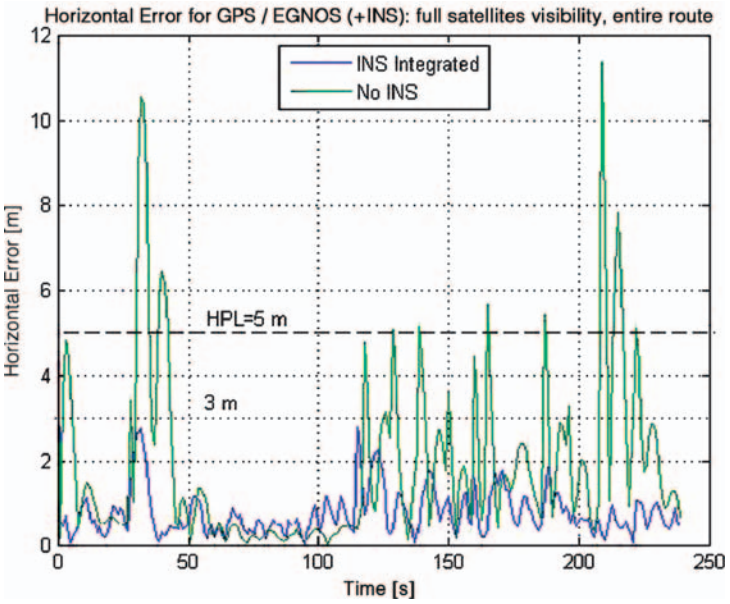

Fig. 6. Performance comparison between GPS / EGNOS receiver and INS-integrated receiver during movement along entire chosen route in case of full satellites visibility.

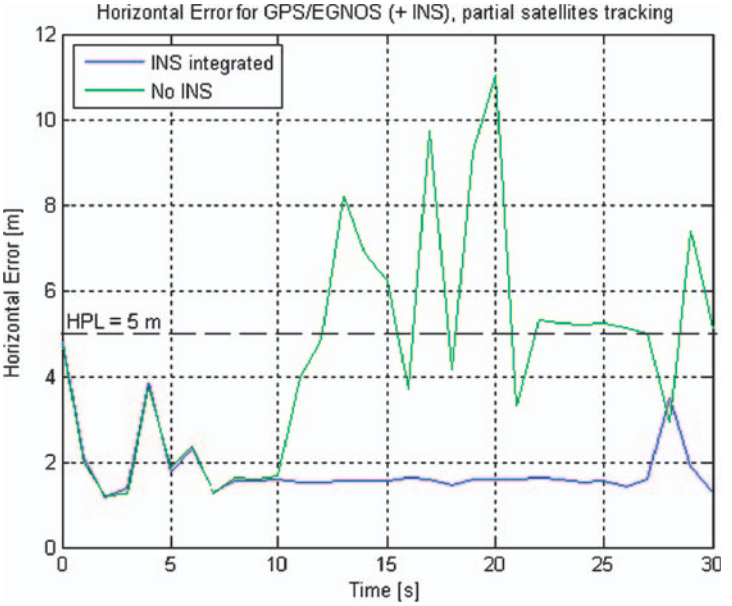

Fig. 7. Performance comparison between GPS / EGNOS receiver and INS-integrated receiver in case of tracking gap of some satellites.

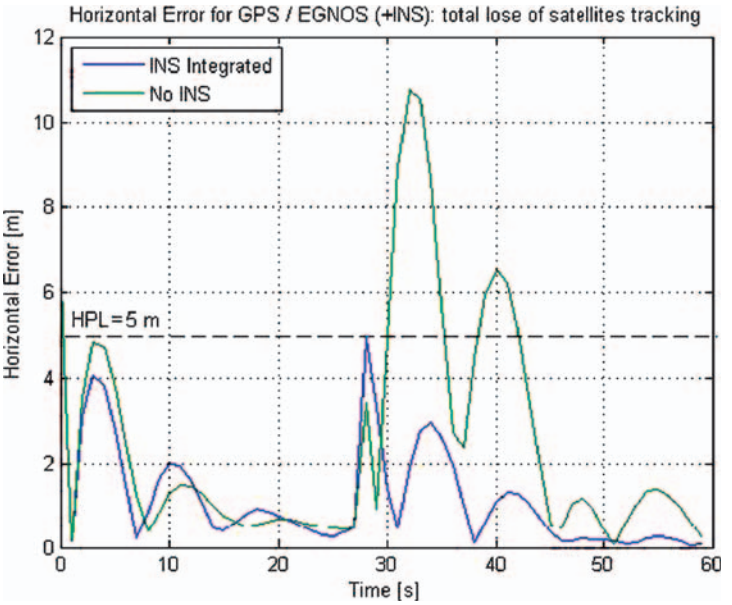

Fig. 8. Performance comparison between GPS / EGNOS receiver and INS-integrated receiver in case of total lose of satellites tracking.

a strong detrimental effect on positioning accuracy. With no integration, the SA is only at 58.1%, and the RMS error is 5.243 m. Our integrated solution is more stable and reliable and presents no discernible degradation, maintaining 100% of service availability and RMS error 1.978 m.

Figure 8 represents an extreme scenario of total loss of tracking of satellites for 20 seconds (20–40): in correspondence of approximately second 28, the vehicle arrives at waypoint 2, and the consequent turn degrades heavily the performance of GPS stand-alone receiver, with error that remains above 5 m for many seconds. Indeed, this is due to the total absence of measurements for correction of the predicted state, which evolves freely in time depending on a mispredicted vehicle dynamic. With support of sensors, the receiver manages to maintain always required performance because of the limited duration of satellites gap, when the sensor measurement errors are not sufficient to degrade position estimation significantly.

5 Conclusions

In this paper we showed that it's possible to augment typical capabilities of GNSS stand-alone receivers with a tightly coupled Kalman filtered integrated solution which uses low cost MEMS sensors of accelerations and rotations. With an expense of a few tens of $, we can equip a terrestrial maintenance vehicle for airport activity with this new hybrid advanced receiver, making feasible an accurate and reliable service of surveillance of overall airport activity for a more efficient ATM. Our hybrid receiver is capable of guarantee an horizontal position estimation error lower than 5 m even in the worst scenarios (high dynamics and bad tracking of satellites) and lower than 3 m (about 1 m) in more common and realistic situations.

References

[1] B. W. Parkinson, J. J. Jr. Spilker, *Global Positioning System: Theory and Applications*, vols. 1 and 2, American Institute of Aeronautics and Astronautics, 370 L'Enfant Promenade, SW, Washington, DC, 1996.

[2] M. S. Grewal, L. R. Weill, A. P. Andrews, *GPS Global Positioning Systems – Inertial Navigation and Integration*, Wiley 2001.

[3] Y. Bar-Shalom, X. Rong Li, T. Kirubarajan, *Estimation with Applications To Tracking and Navigation*, Wiley 2001.

[4] *TIM-LR Sensor-Based GPS Module Data Sheet*, u-blox, 2005.

[5] *Analog Devices ADXL103 and ADXRS150 Data Sheets*, Analog Devices, 2004.

[6] RTCA/DO-229C, *Minimum Operational Performance Standards For Global Positioning System/Wide Area Augmentation System Airborne Equipment*, RTCA Inc., November 28 2001.

[7] J. B.-Y. Tsui, *Fundamentals of Global Positioning System Receivers – A Software Approach*, Wiley, 2005.

[8] J. B. Y. Tsui, M. H. Stockmaster, D. M. Akos, *Block Adjustment of Synchronizing Signal (BASS) for Global Positioning System (GPS) Receiver Signal Processing*, GPS97.

[9] C. T. Brumbaugh, A. W. Love, G. M. Randall, D. K. Waineo, S. H. Wong, *Shaped Beam Antenna for the Global Positioning Satellite System, Rockwell International Corporation*, Antennas and Propagation Society International Symposium, 1976.

[10] F. M. Czopek, S. Shollenberger, *Description and Performance of the GPS Block I and II L-Band Antenna and Link Budget*, GPS93.
[11] *Navstar GPS Space Segment/Navigation User Interfaces, Interface Specification IS-GPS-200, Revision D, November 7 2004*, ARINC Engineering Services, LLC.
[12] *WGS84 Implementation Manual*, EUROCONTROL and Institute of Geodesy and Navigation (IfEN), Version 2.4, February 12 1998.
[13] W. Gurtner, *RINEX: The Receiver Independent Exchange Format Version 2.10*, Astronomical Institute, University of Berne, June 8 2001.